Polarimetric Detection of Objects Buried in Snowpack by a Synthetic Aperture FM-CW Radar

Yoshio Yamaguchi, *Senior Member, IEEE,* and Toshifumi Moriyama

Abstract—**This paper presents experimental results of polarimetric detection of objects buried in a natural snowpack by a synthetic aperture FM-CW radar. First, the principle of polarimetric imaging in the Co- and Cross(X)-pol radar channels is outlined based on the scattering matrix and the characteristic polarization states for a specific target. Then, polarimetric measurements were carried out to detect objects buried in a natural snowpack 230 cm deep. The targets included two orthogonally placed metallic plates, an ice layer within the snowpack, and a human body. It is shown that the polarimetric FM-CW radar clearly enhances target signatures and that it serves to significantly improve detection in snowpack. Several polarimetric detection results are displayed, demonstrating the potential capability of characteristic polarization imaging and the usefulness of FM-CW radar.**

I. Introduction

THERE are many requirements to detect buried objects in regions with heavy snowfall. The typical objects are avalanche victims, guard rails/wires on road shoulders for snow removal, and other general objects which may be buried by blizzards or heavy snowfalls. Ordinarily, these objects are buried to a depth of, at most, a few meters. Microwave subsurface radar is the most suitable tool for these detection problems. This paper extends earlier work [1], [2] and documents enhanced detection of objects buried in snowpack using a polarimetric synthetic aperture FM-CW radar which takes account of full polarimetric information.

Radar polarimetry, i.e., the full utilization of the vector nature of electromagnetic wave information, is an indispensable tool for advanced imaging radar systems [3], [4]. If radar polarimetry is incorporated into a synthetic aperture FM-CW radar system, the radar will have advantages in detection that:

1) it has a potential ability for precisely measuring distances in the near range with considerably simpler equipment than pulsed radar systems;
2) it can provide Sinclair scattering matrix data;
3) hence, it is possible to synthesize polarimetric power; and
4) polarimetric filtering may be applied to the detected image.

Manuscript received September 13, 1994; revised March 24, 1995. This work was supported in part by a Grant-in-Aid for Scientific Research of the Ministry of Education, Japan.

The authors are with the Department of Information Engineering, Faculty of Engineering, Niigata University, Niigata-shi 950-21 Japan.

Publisher Item Identifier S 0196-2892(96)00278-1.

The purpose of this paper is to experimentally show the usefulness of polarimetric FM-CW radar for detection in snowpack. The emphasis is placed on experimental results based on characteristic polarization state imaging of targets buried in a natural snowpack. Polarimetric enhancement factor, defined as the received power ratio of two different targets [5], [6], is employed as a discriminator which enhances one target versus another in the image. It is possible to enhance or completely eliminate one of the targets even in the snow medium by using a characteristic polarization state which optimizes (maximizes or minimizes) the received power or the enhancement factor.

In the following, a brief introduction of a scattering matrix obtained by a polarimetric synthetic aperture FM-CW radar is presented in Section II. Characteristic polarization state imaging as well as polarimetric discrimination of two targets are described in Section III. Section IV displays experimental imaging results of targets buried in an actual snowpack 230 cm deep. The targets are metallic plates, an ice layer within a snowpack, and a human body. Several polarimetric enhanced images are displayed in Section V, demonstrating the potential capability of characteristic polarization imaging and the usefulness of FM-CW radar polarimetry in snowpack.

II. Polarimetric Reflection Coefficients from Synthetic Aperture FM-CW Radar

FM-CW radar determines a target distance by measuring the beat frequency between a transmitted radar signal and the received signal from the target [2]. The transmitted signal is linearly swept from $f_0 - [(\Delta f)/2]$ to $f_0 + [(\Delta f)/2]$ where f_0 is the center frequency. If a target whose reflection coefficient distribution function is given by $g(x_0, z_0)$ is located at a distance r from the transmitting antenna (Fresnel region) in a medium of permittivity ε_r as shown in Fig. 1, the beat spectrum due to the target achieves its maximum at $z \approx z_0$ and can be written [2], [7] as

$$U(x, z_0) = B \int_{-\infty}^{\infty} g(x_0, z_0) h(x - x_0, z_0)\, dx_0 \qquad (1)$$

where B is an amplitude, $g(x_0, z_0)$is a point target reflection coefficient at the position (x_0, z_0), and $h(x - x_0, z_0)$is a

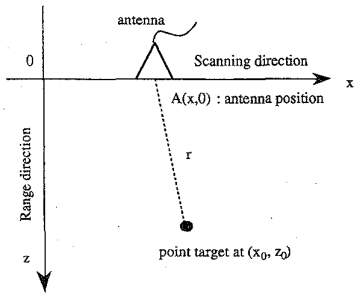

Fig. 1. Position of antenna and a point target.

propagation function given by

$$h(x - x_0, z_0) = \exp\left|j\,\frac{4\pi\sqrt{\varepsilon_r}f_0}{c}\left\{z_0 + \frac{(x - x_0)^2}{2z_0}\right\}\right|. \quad (2)$$

Because of its convolution integral form, $U(x, z_0)$ can be interpreted as a Fresnel hologram. The reflection function can be obtained by an inverse convolution integral [8]

$$g(x_0, z_0) = \int_{-(L/2)}^{L/2} U(x, z_0)h^*(x_0 - x, z_0)\,dx, \quad (3)$$

where L is the antenna-scan width in the x-direction. The symbol $*$ denotes complex conjugation. Equation (3) is the basis for synthetic aperture FM-CW radar, and if L is long enough, it provides a high resolution image in the x-direction (scanning direction) of Fig. 1.

At a constant line of x_0, (3) yields reflection coefficients along the range direction by varying z_0. The incremental interval in range corresponds to the frequency interval in the Discrete Fourier Transform of the beat signal because the beat frequency is proportional to the range z_0. If the sweep frequency bandwidth Δf is chosen wide enough (1.1 GHz in our system) and the number of sampling points in the Fast Fourier Transform is large, the resolution in the range direction is high. Therefore, synthetic aperture FM-CW radar can provide a high resolution two-dimensional (depth and scanning directions) SAR image of a snowpack if the radar is scanned on the surface.

Equation (3) holds for any polarization combination measurement. If we measure $g(x_0, z_0)$ in the conventional (HV) polarization basis, it is possible to obtain complete polarimetric information. In this case, we denote the polarimetric $g(x_0, z_0)$ as g_{HV}. Since the value of g contains amplitude and phase information, we may regard each polarimetric g as the Sinclair scattering matrix element as

$$[S(HV)] = \begin{bmatrix} S_{HH} & S_{HV} \\ S_{VH} & S_{VV} \end{bmatrix} = \begin{bmatrix} g_{HH} & g_{HV} \\ g_{VH} & g_{VV} \end{bmatrix}. \quad (4)$$

Hence, polarimetric synthetic aperture FM-CW radar provides an image consisting of thousands of pixels, each corresponding to a Sinclair scattering matrix [9]. We use this scattering matrix for the polarimetric imaging which follows.

III. Polarimetric Imaging

As mentioned in the previous section, the subsurface polarimetric FM-CW radar provides a two-dimensional SAR image consisting of many pixels with each pixel having a scattering matrix (4). If a scattering matrix (or equivalently a pixel) is given, it is possible to synthesize any polarimetric channel power by using a specific polarization state. The optimization of the received power for a given target is well tabulated in [10].

It is known [10] that there exist physically a total of eight distinct characteristic polarization states for a single target. These polarization states are Co-Pol maximum, Co-Pol extremum, a pair of Co-Pol nulls, a pair of Cross(X)-Pol maximums, a pair of X-Pol saddles, and a pair of X-Pol nulls. Since the Co-Pol maximum and extremum are identical with the X-pol nulls, the total number is eight. The Co-Pol channel implies that the polarization state of the receiver is identical with that of the transmitter, whereas the X-pol channel means the receiver antenna has the polarization state orthogonal to that of the transmitter. For the Co-Pol channel case, the maximum power is obtained by selecting the Co-Pol max polarization state [10] (equivalently the polarization ratio ρ) as

$$\rho_{cm\,1,2} = \frac{-B \pm \sqrt{B^2 - 4AC}}{2A}, \quad (5)$$

where $A = S_{HH}^* S_{HV} + S_{HV}^* S_{VV}$, $B = |S_{HH}|^2 - |S_{VV}|^2$, $C = -A^*$, and S_{ij} is the scattering matrix element. By using this specific polarization ratio, the radar channel power for the selected pixel is always maximized. In general, an SAR image consists of many pixels with different scattering matrices. However, a target may have similar scattering matrices in several pixels within an SAR image that differ from those in other pixels in the image. If we select a representative pixel or scattering matrix pertaining to a target, it is possible to determine Co-Pol max according to (5) and to recalculate the channel power in all other pixels of an SAR image again keeping the target maximized. The resultant image becomes the Co-Pol max image for the target. The same procedure applies to the other characteristic polarization states. This is the characteristic polarization filtering technique for a specific target in SAR imagery.

We apply this principle to the image obtained by the FM-CW radar both in the range and the scanning direction of a lossy inhomogeneous snowpack. However, in the detection problem, there may be several targets within the medium, i.e., a coexistence of several targets embedded (the depth may be different) in a snowpack. In this case, the requirement for the radar is to discriminate these targets. For discrimination of targets, let us define a polarimetric contrast enhancement factor for both channels as below:

$$\text{Co-Pol channel} \quad C_c = \frac{P_1^c}{P_2^c} = \left|\frac{\boldsymbol{h}^{\mathrm{T}}[S]_1\boldsymbol{h}}{\boldsymbol{h}^{\mathrm{T}}[S]_2\boldsymbol{h}}\right|^2, \quad (6)$$

$$\text{X-Pol channel} \quad C_x = \frac{P_1^x}{P_2^x} = \left|\frac{\boldsymbol{h}_\perp^{\mathrm{T}}[S]_1\boldsymbol{h}}{\boldsymbol{h}_\perp^{\mathrm{T}}[S]_2\boldsymbol{h}}\right|^2 \quad (7)$$

where P is the received power in each channel, $[S]$ is the scattering matrix, $\boldsymbol{h}$ is the polarization state of the radar transmitter expressed in terms of the polarization ratio ρ defined by

$$\boldsymbol{h} = \frac{1}{\sqrt{1+\rho\rho^*}}\begin{bmatrix}1\\ \rho\end{bmatrix}, \tag{8}$$

$\boldsymbol{h}_\perp$ is the orthogonal polarization state, the superscript T denotes transpose, and the subscripts 1 and 2 refer to the targets which we wish to maximize and minimize, respectively.

The problem becomes to find a polarization state (i.e., polarization ratio ρ) which maximizes the contrast (6) in a lossy inhomogeneous medium. The maxima of (6) and (7), hence, the corresponding polarization states, may be directly found from

$$C_c = \infty \Rightarrow \boldsymbol{h}^{\mathrm{T}}[S]_2\boldsymbol{h} = 0, \tag{9}$$

$$C_x = \infty \Rightarrow \boldsymbol{h}_\perp^{\mathrm{T}}[S]_2\boldsymbol{h} = 0, \tag{10}$$

which lead (9) and (10) to

$$P_2^c = \left|\frac{S_{2,HH} + 2S_{2,HV}\rho + S_{2,VV}\rho^2}{1+\rho\rho^*}\right|^2 = 0, \tag{11}$$

$$P_2^x = \left|\frac{-S_{2,VH} + S_{2,HV}\rho\rho^* + S_{2,HH}\rho^* - \rho S_{2,VV}}{1+\rho\rho^*}\right|^2 = 0 \tag{12}$$

in the monostatic radar, assuming $S_{2,HV} = S_{2,VH}$. Therefore, the specific polarization states are given by

Co-Pol channel

$$\rho_{cn\,1,2} = \frac{-S_{2,HV} \pm \sqrt{S_{2,HV}^2 - S_{2,HH}S_{2,VV}}}{S_{2,VV}} \tag{13}$$

X-Pol channel

$$\rho_{xn\,1,2} = \frac{-B_2 \pm \sqrt{B_2^2 - 4A_2C_2}}{2A_2} \tag{14}$$

$$A_2 = S_{2,HH}^* S_{2,HV} + S_{2,HV}^* S_{2,VV},$$
$$B_2 = |S_{2,HH}|^2 - |S_{2,VV}|^2,$$
$$C_2 = -A_2^*.$$

It should be noted that (14) is of the same form as (5), i.e., Co-Pol maxes = X-Pol nulls. The polarization states (13) and (14) are essentially identical with the null characteristic polarization states in each channel which minimize the receiving power from the target 2. Since this methodology may be cast into the form of the characteristic polarization filtering technique mentioned above, we refer to this contrast enhancing method as characteristic polarization state imaging.

By using these characteristic polarization states, it is possible to find or discriminate other targets. This optimization is based on the scattering matrix only, no matter what the propagation medium is. In other words, this method uses a final scattering matrix obtained by the FM-CW radar even if a target is buried in a lossy inhomogeneous medium. In general, a target scattering matrix will be deformed by the propagation process in an inhomogeneous medium. However, what we can obtain is the final scattering matrix which is the combination of the target scattering matrix and modifications imposed by the medium. This optimization assumes the scattering characteristics of targets 1 and 2 are dissimilar, i.e., the scattering matrices of $[S]_1$ and $[S]_2$ are different. If they are similar, the optimization procedure becomes different [6]. In such a case, the power ratio formulation would fail to discriminate two targets because the contrast enhancement factor is close to unity.

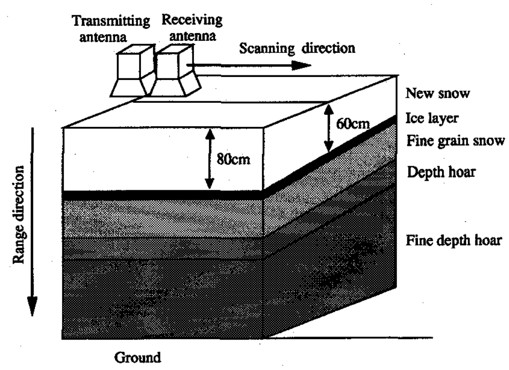

Fig. 2. The structure of snowpack.

IV. Polarimetric Detection in Natural Snowpack

Polarimetric detection experiment of objects in a natural snowpack was carried out to confirm the performance and usefulness of the radar. The radar system was the same one as described in [2] which operates in the frequency range of 1.1–2.2 GHz. The measurement was carried out using dry snowpack on a road shoulder on February 4, 1994, at Yamakoshi village in Niigata Prefecture, Japan. The structure of the natural snowpack is depicted in Fig. 2. This structure was found after the completion of the experiment. It consisted of at least 4 distinct snow layers. The nomenclature of snow type is due to [11]. These layers had a dip angle of 11° oriented perpendicular to the scanning direction. A frozen ice layer was included in the snowpack at 80 cm (at cross section end) to 60 cm deep (beneath the antenna) from the surface, which caused radar clutter due to different permittivity in the snowpack. First, the permittivity of the snowpack was determined by comparing the radar detection range and the actual range. The average permittivity was found to be 1.33, which is a typical value for dry snowpack [12].

The targets used are a metallic plate of 4 × 100 cm which is referred to as target 1 and a metallic plate of 5 × 100 cm (target 2). Fig. 3 shows the experimental situation seen from top and side. These targets were inserted horizontally into the snowpack. Target 1 was buried at a depth of 50 cm, located in the upper left side, while target 2 was buried at 110 cm deep in the lower right side. The two targets were oriented ±45° with

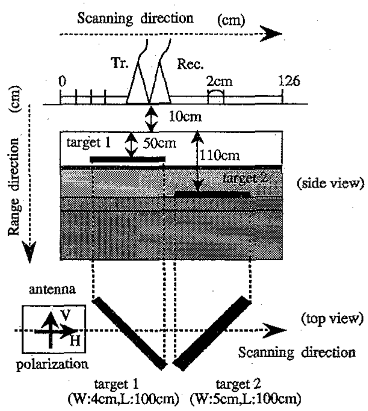

Fig. 3. The experimental situation.

respect to the transmitter polarization and orthogonal to each other as shown in Fig. 3. Polarimetric detection was conducted in the conventional linearly polarized HV basis by changing the direction of horn antennas. In this measurement, H stands for the polarization being parallel to the scanning direction and V for the orthogonal polarization to H. The fixed polarization radar image in Fig. 4 was obtained by scanning the antennas horizontally over the snow surface. The scanning length L was 128 cm and the antenna scanning interval was 2 cm, which yielded 64 points data in the horizontal direction. These images are produced using a synthetic aperture processing [2]. The number of points in the FFT was chosen to be 1024. The range (depth) in Fig. 4 is calibrated according to the measured permittivity. The clutter due to the ice layer around 60 cm deep from the surface is apparent in the Co-Pol (HH and VV) image. However, it is completely suppressed in the X-Pol (HV) image. This is due to the fact that the ice layer behaves like a flat plane. It is interesting to note that the echo strengths from targets 1 and 2 are different, although both targets are oriented $\pm 45°$ with respect to the radar polarization. In the HH image of Fig. 4(a), the echo from target 1 is much smaller than that of target 2, even though the range is closer. This seems to be caused mainly by the inhomogeneity of the propagation medium which may change the original scattering matrix of a target in the propagation process. This is completely different from object detection in free space [5] where the scattering matrix is maintained in the propagation process and the range difference contributes a little in echo strength.

V. Polarimetric Enhanced Image

The combination of polarimetric images of Fig. 4(a)–(c) provides scattering matrices of the same radar scene. The image consists of 64 × 128 pixels in this case. Fig. 5 shows characteristic polarization state images based on polarimetric filtering methodology, i.e., the Co-Pol maximum image for target 1 in Fig. 5(a), the Co-Pol maximum image for target 2 in Fig. 5(b), the Co-Pol minimum image for target 2, i.e., maximum contrast enhanced image for target 1 versus 2 in Fig. 5(c), the Co-Pol minimum image for target 1, the maximum contrast enhanced image for the target 2 versus 1 in Fig. 5(d).

It is seen in Fig. 5(a) that there still exist echoes from target 2 and the ice layer although the target 1 is maximized. The magnitude of target 2 is close to that of target 1. This means the two targets are not orthogonal to each other for the radar in this snow medium. A similar result can be seen in Fig. 5(b) where target 2 is maximized. Fig. 5(a) and (b) correspond to the Co-Pol max characteristic polarization state imaging without considering coexistence of other targets. For a complete discrimination of two targets, i.e., for obtaining maximum contrast of two targets, we have chosen a pixel within target 1 and another pixel in target 2. These pixel locations correspond to the points where the received power for each target is maximum. Then it becomes possible to determine the polarization state according to (6) which nulls the other target. Using the polarization state, we calculated all other pixel values in the entire scene again, resulting in Fig. 5(c). It is seen that target 2 is completely eliminated

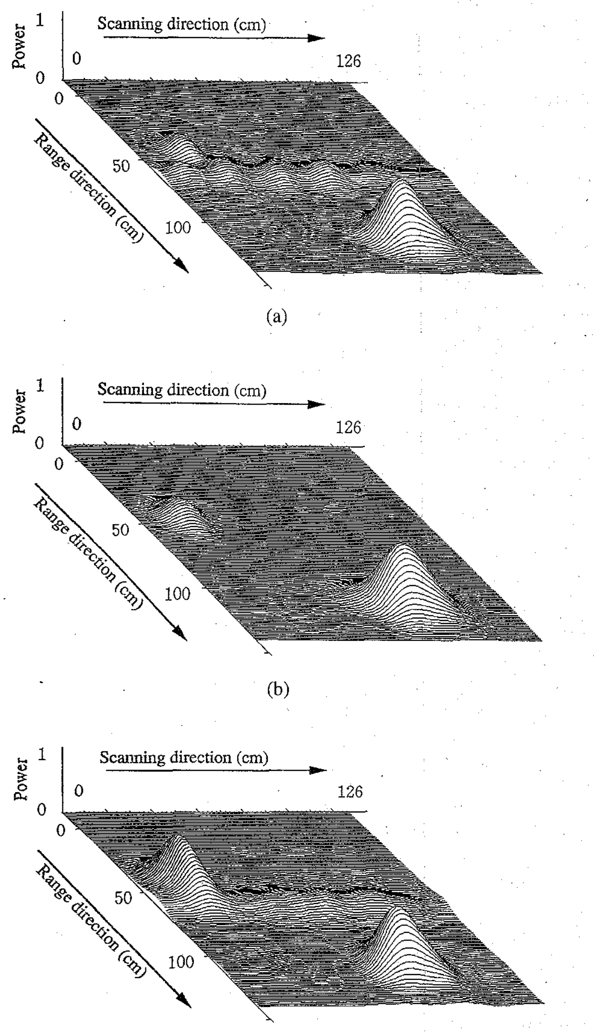

Fig. 4. Fixed polarization images of two metallic plates. (a) HH, (b) HV, and (c) VV.

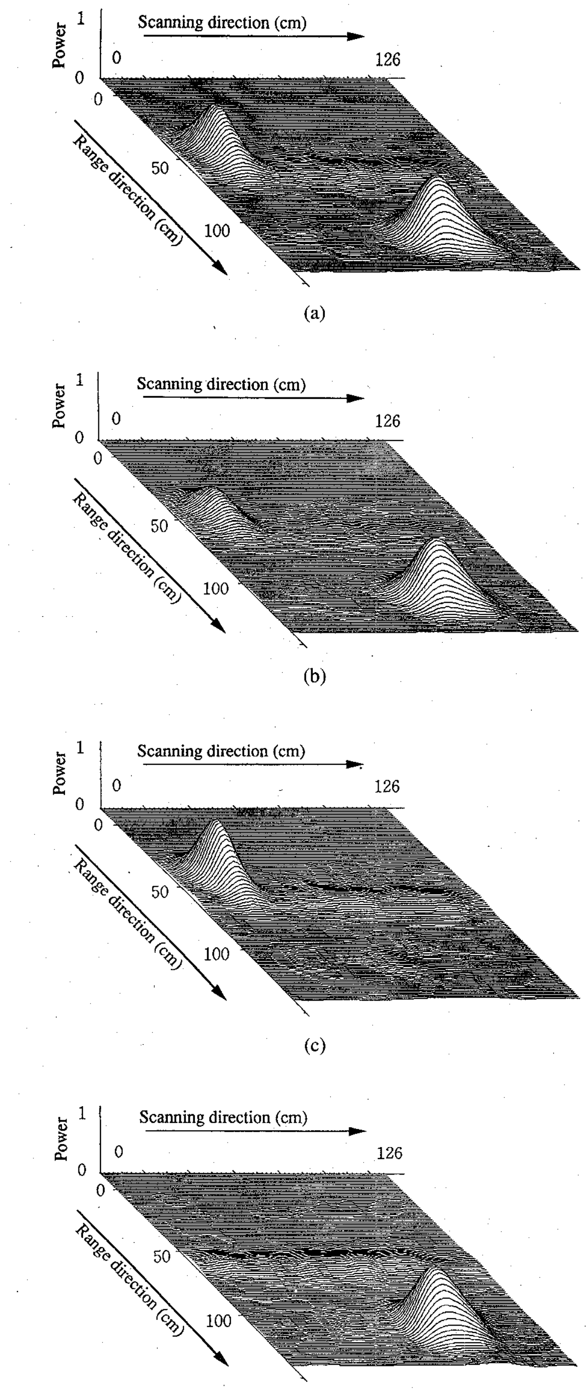

Fig. 5. Polarimetric enhanced images in the Co-Pol channel: (a) Co-Pol max for target 1, (b) Co-Pol max for target 2, (c) Co-Pol null for target 2, and (d) Co-Pol null for target 1.

and target 1 for which we wish to maximize appears strong. Fig. 5(d) displays the reversal case of (c).

The same procedure applies to the X-pol channel images. The final X-Pol null images corresponding to Fig. 5(c) and (d) are shown in Fig. 6(a) and (b). The ice layer is well suppressed, compared to Co-Pol channel images.

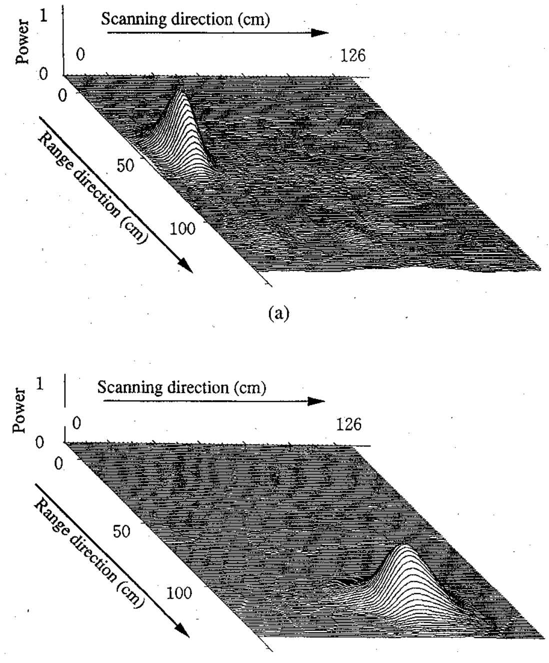

Fig. 6. Polarimetric enhanced images in the X-Pol channel: (a) X-Pol null for target 2 and (b) X-Pol null for target 1.

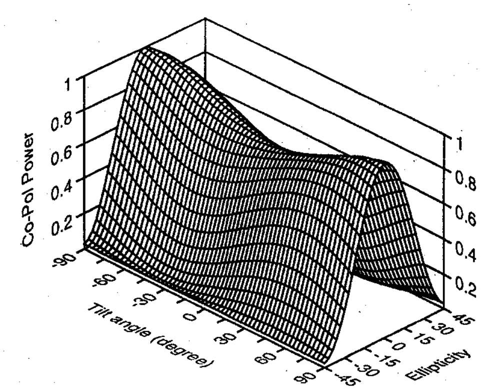

Fig. 7. Polarimetric signature of ice layer in the Co-Pol channel.

The next experiment is to examine the scattering characteristics of the ice layer and enhance the layer within the snowpack. As seen in Figs. 5 and 6, it is better to use *Null* polarization state rather than *Max* polarization state to enhance a specific target. The enhancement requires two targets which have different scattering characteristics. Therefore, we used the same metallic plate of target 2 for the reference. The typical and representative scattering matrix of the ice layer was found to be

$$[S]_{\text{ice}} = \begin{bmatrix} 0.744 - j0.494 & 0.009 + j0.02 \\ 0.009 + j0.02 & 0.971 - j0.24 \end{bmatrix}.$$

The polarimetric power signature is displayed in Fig. 7 indicating that the ice layer behaves like a flat plate [3]. The polarimetric enhanced image of the ice layer is shown in Fig. 8, where Co-Pol max image is in Fig. 8(a) and Co-Pol

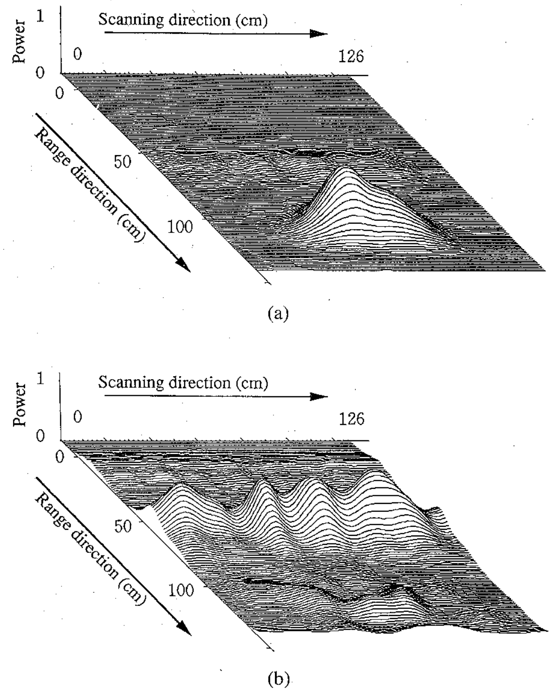

Fig. 8. The polarimetric enhanced image of ice layer: (a) Co-Pol max image and (b) Co-Pol null image of target 2.

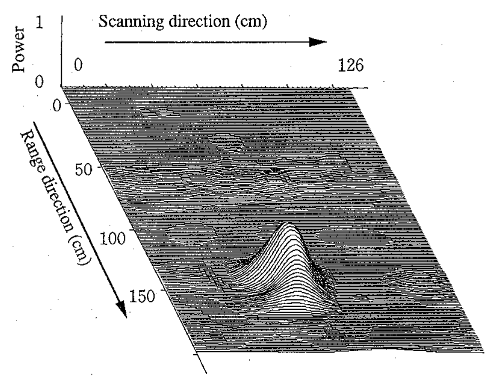

Fig. 9. Co-Pol max image of human body.

null image for the reference target 2 is in Fig. 8(b). The ice layer is much enhanced in Fig. 8(b) and it is easy to recognize that the echo is from a continuous layer because it extended from the left to the right in the image.

The next target is one of the authors. He laid horizontally in a small pit at a depth of 140 cm. Fig. 10 shows the experimental scene. The Co-Pol max image of him only is displayed in Fig. 9. It is seen that the radar can clearly detect the human body.

In summary, if the scattering behavior of targets is different (as it usually is), it is always possible to eliminate one target. This elimination enhances desired target clearly in the SAR image. However, enhancement of a specific target becomes difficult in the presence of multiple targets or heavy inhomogeneity within propagation medium if the scattering characteristics of these targets or inhomogeneity are similar.

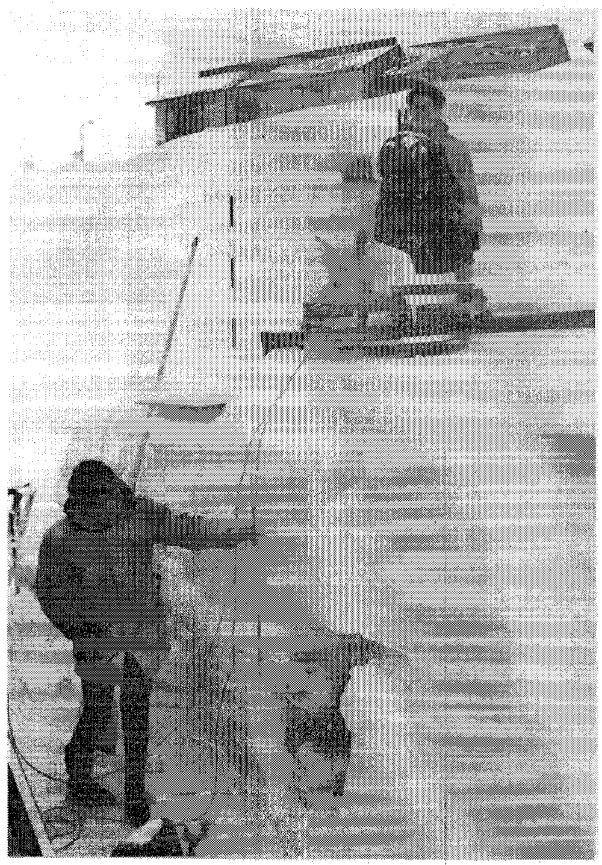

Fig. 10 The experimental scene of human body detection.

The present technique will yield a fine result if the scattering nature of a specific target is different from others. In addition, the polarization state which nulls or maximizes a specific target may be useful for target identification.

VI. Conclusion

This paper demonstrated experimental detection results of objects buried in an actual snowpack by polarimetric synthetic aperture FM-CW radar. The polarimetric filtering principle using the characteristic polarization states for a target was applied to enhance or eliminate a target, resulting in a discrimination of two targets. By using a null characteristic polarization state which minimizes one of targets, it was possible to enhance the other target clearly in a radar image. Even though the propagation medium is inhomogeneous, this methodology can be applied to target discrimination provided the scattering characteristics are different. The polarization state which nulls or maximizes a specific target may be useful for obtaining target information and target identification, which still needs further investigation.

Acknowledgment

The authors are grateful to T. Nakanishi for assisting in the measurements.

REFERENCES

[1] Y. Yamaguchi, M. Mitsumoto, M. Sengoku, and T. Abe, "Human body detection in wet snowpack by an FM-CW radar," *IEEE Trans. Geosci. Remote Sensing,* vol. 30, no. 1, pp. 186–189, Jan. 1992.

[2] ——, "Synthetic aperture FM-CW radar applied to the detection of objects buried in snowpack," *IEEE Trans. Geosci. Remote Sensing,* vol. 32, no. 1, pp. 11–18, Jan. 1994.

[3] J. A. Kong, Ed., *PIER3 Progress in Electromagnetics Research.* Amsterdam: Elsevier, 1990.

[4] W.-M. Boerner *et al., Direct and Inverse Methods in Radar Polarimetry, Parts 1 and 2,* NATO ASI Series C: Mathematical and Physical Sciences, vol. 350. Norwell, MA: Kluwer, 1992.

[5] P. Dubois and J. J. van Zyl, "Polarization filtering of SAR data," *SPIE, Radar Polarimetry,* vol. 1748, pp. 309–320, 1992.

[6] A. B. Kostinski and W.-M. Boerner, "On the polarimetric contrast optimization," *IEEE Trans. Antennas Propagat.,* vol. AP-35, no. 8, pp. 988–991, 1987.

[7] J. W. Goodman, *Introduction to Fourier Optics.* New York: McGraw-Hill, 1968.

[8] Y. Aoki, *Wave Signal Processing.* Tokyo: Morikita Syuppan, 1986.

[9] H. Mott, *Antennas for Radar and Communications.* New York: Wiley, 1992.

[10] W.-M. Boerner, W. L. Yan, A. Q. Xi, and Y. Yamaguchi, "On the basic principles of radar polarimetry: The target characteristic polarization state theory of Kennaugh, Huynen's polarization fork concept and its extension to the partially polarized case," *Proc. IEEE,* vol. 79, no. 10, pp. 1538–1550, Oct. 1991.

[11] *The International Classification for Snow: CRREL Part II, Physical Science,* sec. B, pp. 19–28, July 1962.

[12] F. T. Ulaby, R. K. Moore, and A. K. Fung, *Microwave Remote Sensing—Active and Passive,* vol. III. Norwood, MA: Artech House, 1986.

[13] Y. Yamaguchi, T. Nishikawa, M. Sengoku, W.-M. Boerner, and H. J. Eom, "Fundamental study on synthetic aperture FM-CW radar polarimetry," *IEICE Trans. Commun.,* vol. E77-B, no. 1, pp. 73–80, Jan. 1994.

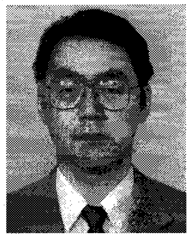

Yoshio Yamaguchi (M'83–SM'94) was born in Niigata, Japan, on March 12, 1954. He received the B.E. degree in electronics engineering from Niigata University in 1976, and the M.E. and Dr.Eng. degrees from Tokyo Institute Technology, Tokyo, Japan, in 1978 and 1983, respectively.

In 1978, he joined the Faculty of Engineering, Niigata University, where he is a Professor. During 1988–1989, he was a Research Associate at the University of Illinois at Chicago. His interests are in the field of propagation characteristics of electromagnetic waves in lossy medium, radar polarimetry, microwave remote sensing, and imaging.

Dr. Yamaguchi is a member of IEICE of Japan and the Japan Society for Snow Engineering.

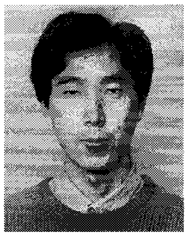

Toshifumi Moriyama was born in Fukui Prefecture, Japan, on January 1, 1972. He received the B.E. degree in information engineering from Niigata University in 1994.

He is now a graduate student in Niigata University where he is engaged in polarimetric radar sensing of buried objects.

Mr. Moriyama is a student member of the Institute of Electronic, Information, and Communication Engineers (IEICE) of Japan.